

Memory effects in microscopic traffic models and wide scattering in flow-density data

Martin Treiber* and Dirk Helbing†

Institute for Economics and Traffic, Dresden University of Technology, Andreas-Schubert-Strasse 23, 01062 Dresden, Germany

(Received 18 April 2003; published 21 October 2003)

By means of microscopic simulations we show that noninstantaneous adaptation of the driving behavior to the traffic situation together with the conventional method to measure flow-density data provides a possible explanation for the observed inverse- λ shape and the wide scattering of flow-density data in “synchronized” congested traffic. We model a memory effect in the response of drivers to the traffic situation for a wide class of car-following models by introducing an additional dynamical variable (the “subjective level of service”) describing the adaptation of drivers to the surrounding traffic situation during the past few minutes and couple this internal state to parameters of the underlying model that are related to the driving style. For illustration, we use the intelligent-driver model (IDM) as the underlying model, characterize the level of service solely by the velocity, and couple the internal variable to the IDM parameter “time gap” to model an increase of the time gap in congested traffic (“frustration effect”), which is supported by single-vehicle data. We simulate open systems with a bottleneck and obtain flow-density data by implementing “virtual detectors.” The shape, relative size, and apparent “stochasticity” of the region of the scattered data points agree nearly quantitatively with empirical data. Wide scattering is even observed for identical vehicles, although the proposed model is a time-continuous, deterministic, single-lane car-following model with a unique fundamental diagram.

DOI: 10.1103/PhysRevE.68.046119

PACS number(s): 89.40.-a, 05.60.-k, 05.70.Fh, 47.55.-t

I. INTRODUCTION

The nature of “synchronized” traffic flow is one of the most controversial subjects in traffic theory [1,2]. It is a form of congested traffic with nonzero flows typically found upstream of inhomogeneities (e.g., freeway bottlenecks), and characterized by an erratic motion of time-dependent flow-density data in a two-dimensional area (with a synchronization of the time-dependent average vehicle velocities among neighboring lanes) [3–5].

The wide scattering of the data points for congested traffic seems to exclude explanations in terms of traffic models assuming a fundamental (steady-state) relation $Q_c(\rho)$ between the flow Q and the density ρ . In response, models with non-unique flow-density relations (or velocity-distance relations) have been proposed on a macroscopic level [6], as car-following models [7–10], and as cellular automata [11]. The empirical data scattering has also triggered a flood of publications in physics journals with various other suggestions ranging from shock waves propagating forward or backward [3], effects of lane changing, changes in the behavior of “frustrated” drivers [12–14], anticipation effects [15,16], or a trapping of vehicles [17]. Another possible explanation of the scattering lies in the heterogeneity of vehicles (such as cars and trucks) and driving styles (such as defensive or aggressive) on any real road [18,19]. In fact, statistical analyses of single-vehicle data show a particularly wide scattering of the time gaps between successive vehicles in congested traffic [20–22]. Furthermore, the average time gaps increase in congested traffic suggesting that “frustration effects” are real

[22]. Macroscopic simulations taking into account observed variations in the truck percentage [19] or direct microsimulations with two types of vehicles [23] could explain a great deal of the observed scattering, but the two-dimensional (2D)-regions remained somewhat smaller than in the observed data.

Another factor possibly contributing to the wide scattering is traffic instabilities which often lead to nonstationary congested traffic such as “oscillating congested traffic.” In fact, at least in Germany, this type of congestion is the most common form of congested traffic [24]. If the sampling time interval for data aggregation is not commensurable with the frequency of the oscillations or if the oscillations are nonperiodic, then the data points will display artificial “erratic scattering.” In this case, the origin of scattering is the method of data aggregation in combination with the conventional interpretation of flow-density data [18].

In this paper we show by means of simulations that the adaptation of drivers to the surrounding traffic on time scales of a few minutes (the “memory effect”) offers a possible quantitative explanation of the observed scattering in conjunction with traffic instabilities. Our model is based on the observation that, after being stuck for some time in congested traffic, most drivers adapt their driving style, e.g., by increasing their preferred *netto* (bumper-to-bumper) time gap T to the preceding vehicle [2,20–22]. Apart from congestion, other aspects of the traffic environment such as driving in the dark or in tunnels affect the driving behavior as well [25], but will not be considered in this paper.

Models based on memory effects have been successfully applied in several fields of statistical and interdisciplinary physics such as liquid crystals and polymers [26] or in reaction-diffusion systems [27]. Moreover, nonlinear Markov equations with memory kernel have been applied to multiple-agent systems and financial markets and provide a

*Electronic address: martin@mtreiber.de;

URL: <http://www.mtreiber.de>

†Electronic address: helbing@trafficforum.org;

URL: <http://www.helbing.org>

statistical mechanism for the observed clustered volatility [28].

In the following section, we formulate the adaptation of the driving style to the surrounding traffic and incorporate memory effects into the intelligent-driver model (IDM) [24] resulting in the IDMM (“intelligent-driver model with memory”). As the IDM, the IDMM is a deterministic time-continuous car-following model with a unique steady-state flow-density relation.

In Sec. III, we present related simulations and compare the measurements of “virtual detectors” with empirically measured traffic data. We find a semiquantitative agreement. While the scattering is even observed in the original IDM, the memory effect is necessary to obtain the inverse- λ shape and the correct relative size of the two-dimensional region of data scattering.

In Sec. IV we discuss under which circumstances can erratic scattering be obtained from deterministic single-lane models with a unique fundamental diagram in simulations without any element of stochasticity or heterogeneity.

II. MODEL EQUATIONS

We will formulate the memory effect in human driver behavior in a way that directly connects to existing car-following models. In principle, any model can be used, the parameters of which can be interpreted in terms of the driving behavior. The model should allow to define some desired velocity v_0 and to influence the minimum netto time gap T by varying one or more of its model parameters. The outcome, of course, will depend on the details of the model used. In this paper, we apply the IDM [24] as the underlying model, where v_0 and T are model parameters themselves.

A. The intelligent-driver model

In the IDM, the acceleration of each vehicle α is assumed to be a continuous function of the velocity v_α , the netto distance gap s_α , and the velocity difference (approaching rate) Δv_α to the leading vehicle:

$$\dot{v}_\alpha = a \left[1 - \left(\frac{v_\alpha}{v_0} \right)^4 - \left(\frac{s^*(v_\alpha, \Delta v_\alpha)}{s_\alpha} \right)^2 \right]. \quad (1)$$

This expression is an interpolation of the tendency to accelerate with $a_f(v) := a[1 - (v/v_0)^4]$ on a free road and the tendency to brake with deceleration $-b_{\text{int}}(s, v, \Delta v) := -a(s^*/s)^2$, when vehicle α comes too close to the vehicle in front. The deceleration term depends on the ratio between the effective “desired minimum gap” s^* and the actual gap s_α , where the desired gap

$$s^*(v, \Delta v) = s_0 + vT + \frac{v\Delta v}{2\sqrt{ab}} \quad (2)$$

is dynamically varying with the velocity. The first term s_0 on the right-hand side denotes the small minimum distance kept in standing traffic. The second term corresponds to following the preceding vehicle with a constant “safety” netto time gap

T . The third term is only active in nonstationary traffic and implements an accident-free “intelligent” driving behavior including a braking strategy that, in nearly all situations, limits braking decelerations to the “comfortable deceleration” b .

B. Adaptation of the driving style and memory effect

We assume that adaptations of the driving style are controlled by a single internal dynamical variable $\lambda_\alpha(t)$ (the “subjective level of service”), which can take on values between 0 (in standing traffic) and 1 (on a free road), and which relaxes to the instantaneous level of service $\lambda_0(v)$ with a relaxation time τ according to

$$\frac{d\lambda_\alpha}{dt} = \frac{\lambda_0(v_\alpha) - \lambda_\alpha}{\tau}. \quad (3)$$

This means, for each driver the subjective level of service is given by the exponential moving average (EMA) of the instantaneous level of service experienced in the past:

$$\lambda_\alpha(t) = \langle \lambda_{0\alpha} \rangle_{\text{EMA}} = \int_0^t \lambda_0(v_\alpha(t')) e^{-(t-t')/\tau} dt'. \quad (4)$$

We have assumed the instantaneous level of service $\lambda_0(v)$ to be a function of the actual velocity $v(t)$. Obviously, $\lambda_0(v)$ should be a monotonically increasing function with $\lambda_0(0) = 0$ and $\lambda_0(v_0) = 1$. In this paper, we specify the most simple “level-of-service function” satisfying these conditions:

$$\lambda_0(v) = \frac{v}{v_0}. \quad (5)$$

Notice that this equation reflects the level of service or efficiency of movement from the driver’s point of view, with $\lambda_0 = 1$ meaning zero hindrance and $\lambda_0 = 0$ meaning maximum hindrance. (A related parameter, by the way, determines the impatience, nervousness, or degree of panic $1 - \lambda_\alpha$ of pedestrians α , see Ref. [1]). If one models heterogeneous traffic, where different drivers have different desired velocities, there is no “objective” level of service, only an individual and an average one.

Having defined how the traffic environment influences the degree of adaptation λ_α of each driver, we now specify how this internal variable influences the driving behavior. A behavioral variable that is both measurable and strongly influencing the traffic dynamics is the netto time gap T . Figure 1(a) shows that, in congested traffic, the whole distribution of time gaps is shifted to the right compared to data of free traffic [22]. Notice that an increase of the time headway for jammed traffic has been also observed if “jammed traffic” is defined by a density threshold ($\rho > 30$ veh./km/lane) instead of a velocity threshold [20,29]. We model this increase by varying the corresponding IDM parameter in the range between T_0 (free traffic) and $T_{\text{jam}} = \beta_T T_0$ (traffic jam) according to

$$T(\lambda) = \lambda T_0 + (1 - \lambda) T_{\text{jam}} = T_0 [\beta_T + \lambda(1 - \beta_T)]. \quad (6)$$

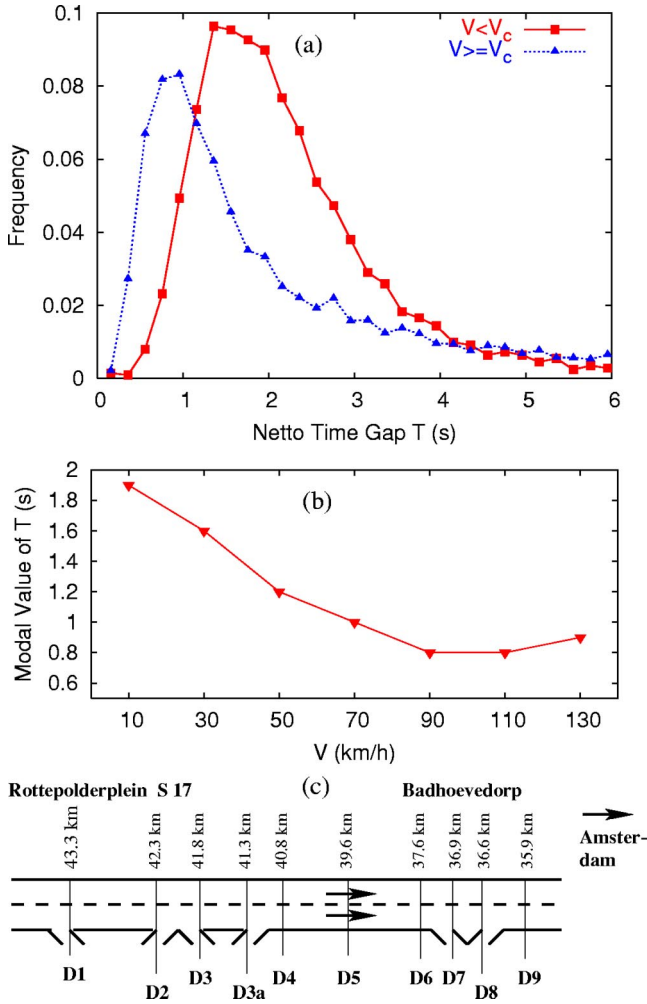


FIG. 1. (a) Distribution of netto time headways on the left lane of cross section D2 of the Dutch A9 from Haarlem to Amsterdam for free traffic ($v > v_c = 60$ km/h) and congested traffic ($v < v_c$). The evaluated dataset contains 15 workdays with several jams. (b) The modal value (most probable value) of the netto time gap for various velocity ranges. The width of the velocity classes is $\Delta v = 20$ km/h, the resolution of the time headways in each class is $\Delta T = 0.1$ s. (c) Sketch of the freeway.

Herein, the *adaptation factor* β_T is a model parameter (cf. Table I). Notice that probably other parameters of the driving style are influenced as well, such as the acceleration a , the comfortable deceleration b , or the desired velocity v_0 . This could be implemented by analogous equations for a , b , and v_0 , respectively. For simplicity (and in order to have an empirically testable model), we will only consider the influence on T .

In summary, the IDMM is defined by the IDM equations (1) and (2), by Eq. (6) describing how the subjective level of service λ influences the time gap, and by the dynamical equation for the internal state itself, which can be written as

$$\frac{d\lambda_\alpha}{dt} = \frac{v_\alpha/v_0 - \lambda_\alpha}{\tau}. \quad (7)$$

The IDMM parameters are intuitive and can be determined from traffic data. In the special case $\beta_T = 1$, the IDMM re-

TABLE I. Model parameters of the IDMM with the values used throughout this paper. All eight model parameters have a clear vehicle- or driver-related meaning and can be determined from empirical traffic data.

Parameter	Typical value
Desired velocity v_0	120 km/h
Netto time gap T_0	0.85 s
Maximum acceleration a	0.8 m/s ²
Comfortable deceleration b	1.8 m/s ²
Minimum distance s_0	1.6 m
Effective vehicle length $l = 1/\rho_{\max}$	6 m
Adaptation factor $\beta_T = T_{\text{jam}}/T_0$	1.8
Adaptation time τ	600 s

verts to the original IDM. The special case $\tau = 0$ corresponds to a slightly modified IDM, where the parameter T in Eq. (2) is replaced by $T(v) = T_0[\beta_T + v/v_0(1 - \beta_T)]$. Table I gives the values that we will use throughout the rest of this paper unless stated otherwise.

Notice that the IDMM belongs to the class of models with a unique stationarity relation. Its steady-state following distance as a function of the velocity is given by

$$s_e(v) = \frac{s_0 + vT_0 \left(\beta_T + (1 - \beta_T) \frac{v}{v_0} \right)}{\sqrt{1 - \left(\frac{v}{v_0} \right)^4}}. \quad (8)$$

Figure 2 shows the resulting fundamental diagram for identical vehicles for the IDMM in comparison with that of the IDM.

III. SIMULATIONS

We have simulated a 20-km-long road section with a bottleneck and open boundaries, assuming identical vehicles of effective length $l = 6$ m whose drivers behave according to the IDMM with the parameters given in Table I. The simu-

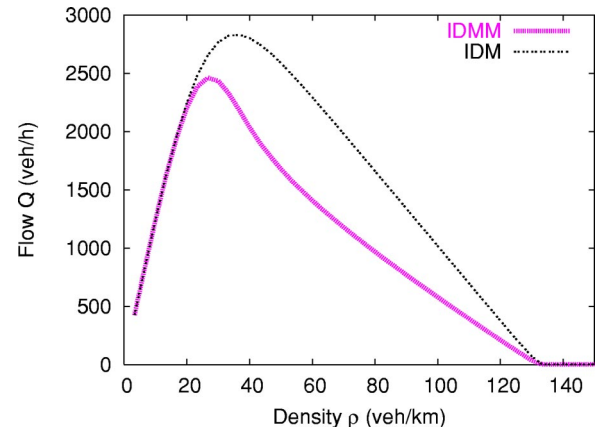


FIG. 2. Comparison of the theoretical fundamental diagrams of the IDM and the IDMM.

lations have been started with very light traffic corresponding to a homogeneous density of 2 veh/km and an initial velocity of 100 km/h. During the simulated time interval of 3 h, we have simulated idealized rush-hour conditions by increasing the inflow at the upstream boundary linearly from 200 veh/h at $t=0$ to 2400 veh/h at $t=25$ min. Afterwards, the flow has been decreased linearly to 100 veh/h at $t=180$ min. All vehicles have been initialized with $\lambda_\alpha(0) = 1$, i.e., with an assumed “memory” of free traffic. As in macroscopic traffic simulations of open systems [30], the velocity of the inflowing traffic turned out to be irrelevant, since it quickly approached the value corresponding to the “free” branch of the velocity-flow relation $v_\alpha(Q)$ with a flow $Q(t)$ equal to that imposed at the boundary.

We have implemented a flow-conserving bottleneck by locally increasing the IDM parameter T_0 ,

$$T_0 = T_0(x) = \begin{cases} 1.20 \text{ s}, & 17 \text{ km} \leq x < 18 \text{ km} \\ 0.85 \text{ s}, & \text{otherwise.} \end{cases} \quad (9)$$

This corresponds to lowering the road capacity and is representative for any bottleneck which is not an on- or off-ramp [32]. Notice that, at the bottleneck, this means that the actual time headway T , as specified by Eq. (6) with (9), depends both directly on x and on the subjective level of service of the driver resulting in another indirect dependence on x .

The simulation has been performed using Euler integration for the velocity and second-order time steps (using the average of the old and new velocities) for the update of the positions [31]. Output is produced by implementing “virtual detectors” at $x=9$ km and $x=12$ km, with data aggregation periods of $T_{\text{aggr}}=60$ s. In each aggregation interval i , the traffic flow

$$Q_i = n_i / T_{\text{aggr}} \quad (10)$$

is determined by counting the number n_i of crossing vehicles. As in many practical cases, the average velocity V_i is calculated as the arithmetic average

$$V_i = \frac{1}{n_i} \sum_{\alpha=1}^{n_i} v_\alpha, \quad (11)$$

and the density as

$$\rho_i = Q_i / V_i. \quad (12)$$

Figure 3 displays the resulting flow-density data of the two virtual detectors, compared with empirical data from real traffic. Both diagrams show (i) the characteristic wide and erratic scattering of the data points which is a signature of “synchronized traffic,” (ii) the characteristic inverse- λ shape with a maximum traffic flow Q_{max} in free traffic (immediately prior to the breakdown), which is significantly higher than the typical flows Q_{CT} in the congested traffic after breakdown.

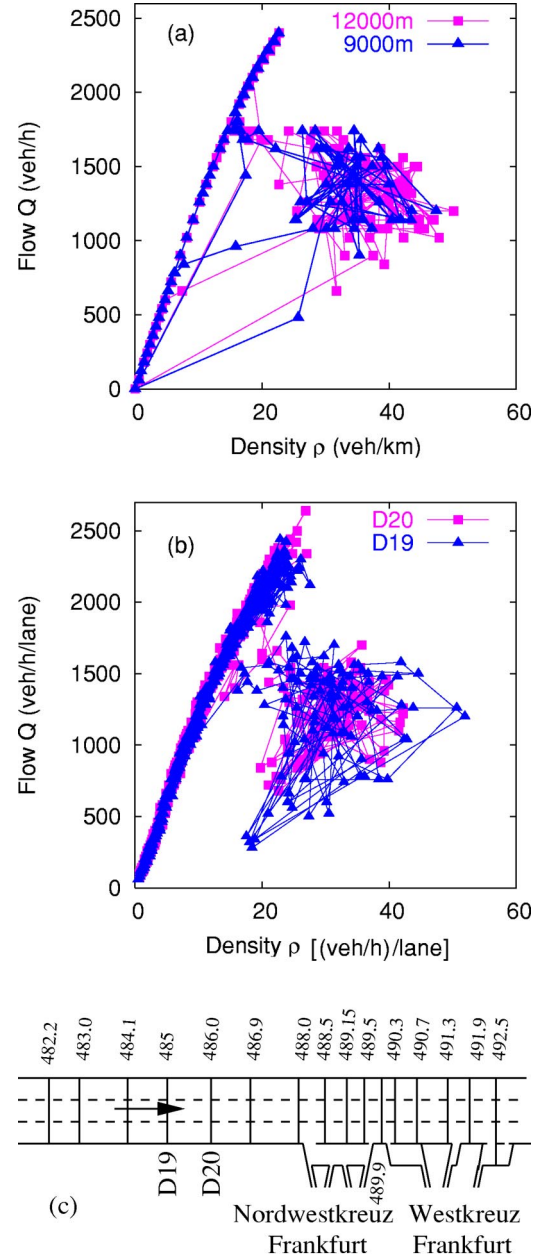


FIG. 3. (a) Simulated flow-density data of two virtual detectors compared with (b) flow-density data from the German freeway A5-South near Frankfurt. The density has been determined by the relation $\rho = Q/V$ with Q being the lane average of the flows and V the lane average of the velocities, weighted with the flow on each lane. Aggregation intervals with zero-vehicle counts have been omitted. (c) Location of the detectors measuring empirical data. Here, the freeway intersection “Nordwestkreuz” plays the role of a bottleneck.

A. Interpretation of macroscopic traffic data

The question arises what causes the obvious stochasticity in the data of the virtual detectors although everything in the simulation is deterministic (including the upstream boundary condition and the implementation of the bottleneck), although all drivers and vehicles are treated identically, and not even lane changes may serve as possible source for fluctua-

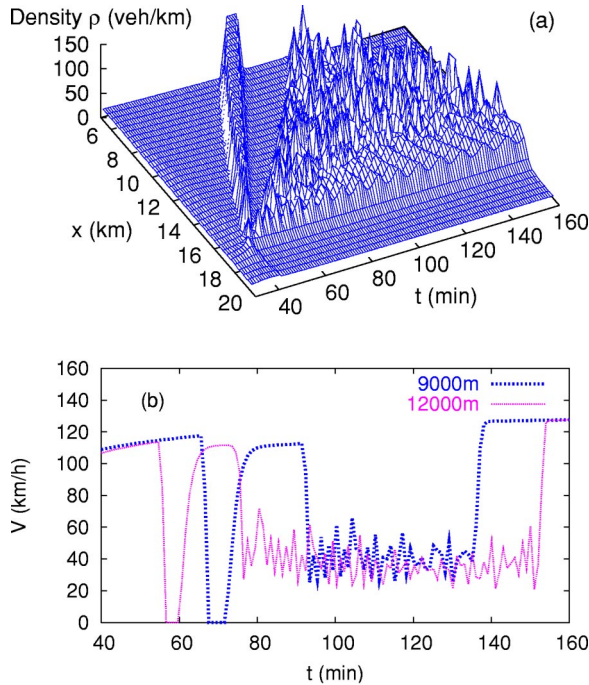


FIG. 4. (a) Spatiotemporal dynamics of the traffic density and (b) time series of the velocity at the two virtual detectors of the simulation shown in Fig. 3.

tions. The only possible source of the fluctuations is traffic instabilities which we will analyze in the following. Figure 4(a) shows that at about $t=40$ min, a traffic breakdown occurs near the bottleneck at $x=17$ km, triggering one isolated wide jam with zero flow and a region of congested traffic with nonzero flow upstream of the bottleneck. In the congested region, initially small oscillations behind the bottleneck (oscillating congested traffic, OCT) increase in amplitude while traveling further upstream [33]. The time series of the virtual detectors [see Fig. 4(b)] show that the wide jam also crosses the detectors. Since the jam and the oscillations of the OCT state are the only possible sources of fluctuations, the scattering in the data of the virtual detectors obviously can be traced back to longitudinal instabilities in connection with the interpretation of the macroscopic data.

Based on theoretical investigations [3], one might expect a “jam line” in the flow-density diagram of Fig. 3, stemming from the wide jam crossing the virtual detectors. However, the jam line is missing (as in most empirical data). Moreover, the highest “measured” density is only about 50 veh/km, although the model parameters (Table I) imply a jam density of at least $\rho_{\text{jam}} = 1/(l + s_0) = 130$ veh/km.

To check whether this is an artifact of the data interpretation, in Fig. 5 we have plotted the flow-density diagram of the same simulation at the same locations. However, instead of determining the macroscopic density via Eq. (12), this time we have used the formula

$$\rho(x, t) = \frac{1}{x_{\alpha-1}(t) - x_{\alpha}(t)} \quad (13)$$

for the actual local density, which one would obtain as “snapshots” at fixed times. Here, the respective vehicle in-

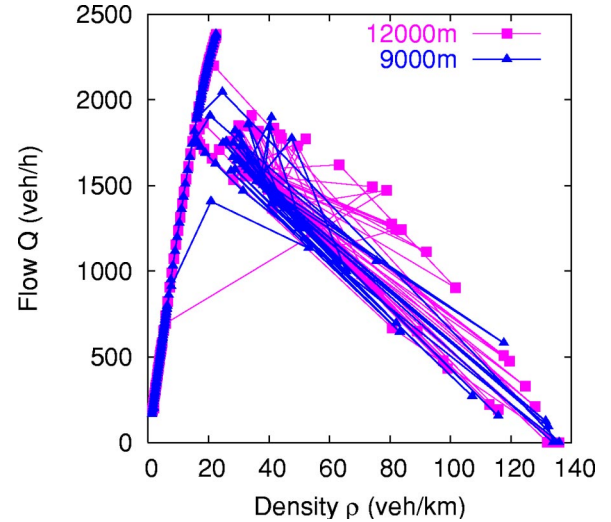


FIG. 5. Flow-density plot as in Fig. 3, but using no data aggregation and the actual local density determined via formula (13).

dex α is given by the condition $x_{\alpha} \leq x < x_{\alpha-1}$. Furthermore, we have defined the instantaneous flow by $Q(x, t) = \rho(x, t)V(x, t)$ with V being the average velocity of the vehicles α and $(\alpha-1)$. In the data for $x=9$ km, one clearly sees the signatures of the fully developed jam in form of a straight jam line J , connecting the points $(\rho_{\text{jam}}, Q_{\text{jam}}) = (130 \text{ veh/km}, 0)$ and $(\rho_{\text{out}}, Q_{\text{out}}) = (18 \text{ veh/km}, 1750 \text{ veh/h})$. Notice that, in accordance with observations [33], the outflow from isolated jams is distinctively lower than Q_{max} . Moreover, the data at both locations show more than one instance of zero or nearly zero flow at densities near the maximum density, which can neither be seen in the time series of the flow-density data nor in those of the velocity, when they are obtained by virtual detectors by means of conventional aggregation of single-vehicle data, cf. Figs. 3 and 4. The reason is that the virtual detectors display finite velocities and flows whenever at least one car crosses the detector during the sampling time interval. Thus, periods of standing traffic of up to the double sampling time, i.e., up to 2 min, may not be observed in the detector output.

If we assume that the simulation captures some essential aspects of real traffic we conclude that (i) a jam line probably exists in real traffic but cannot be found in flow-density data of stationary detectors, (ii) when looking only at aggregated traffic data, one might get a wrong picture of the actual traffic dynamics.

B. Analysis of the adaptation effect

We now proceed to investigate the effects of the new IDMM parameters. We have simulated the same system of equations with various values of the adaptation factor β_T and the adaptation time τ . It turned out that both the outflow Q_{out} from congested traffic (i.e., the downstream flow) and the flow Q_{CT} inside of the congested region decrease with β_T , while the maximum flow Q_{max} essentially remains unchanged. This is plausible, since $(\beta_T - 1)$ describes the strength of the “frustration effect” after driving in congested

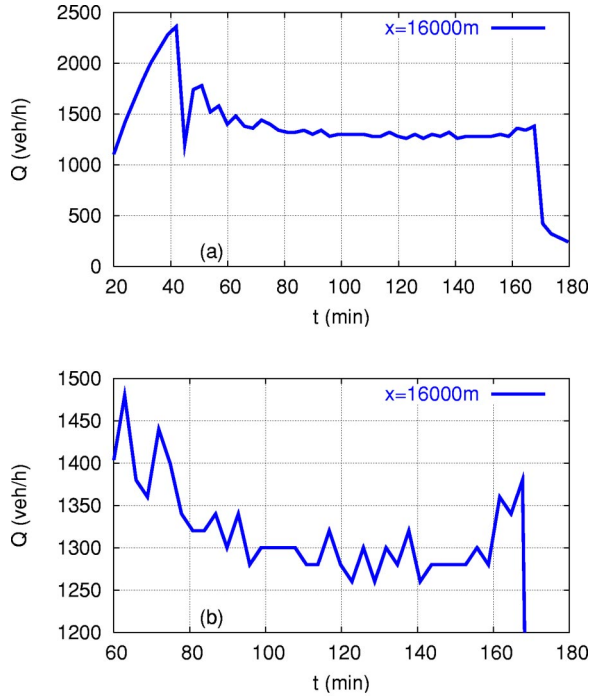


FIG. 6. Time series of traffic flow for the simulation of Fig. 4, measured by a virtual detector at $x = 16\,000$ m near the bottleneck using 3-min sampling intervals. (a) The dip at about $t = 45$ min corresponds to the developing isolated jam while the peak of 1750 veh/h at $t \approx 50$ min is related to the outflow from this jam. (b) Detail of the period of extended congested traffic between $t = 60$ min and $t = 170$ min.

traffic for some time, while the value of Q_{\max} is related to free traffic where frustration effects play a minor role. Furthermore, Q_{CT} decreases with τ . Since the time spent in congestion behind bottlenecks is typically of the order of the adaptation time or longer, drivers are more adapted to congested traffic conditions when they get closer to the downstream front of the congestion area near the bottleneck. (One could also say, they are more frustrated, which may originate from reduced attention due to an exhaustion effect.) Consequently, it takes some time to revert to the more “aggressive” driving style in free traffic, explaining the decrease of Q_{out} with τ .

One might argue that the drivers should adapt instantaneously to the traffic situation. There is empirical evidence, however, that the characteristic time scale for adaptation is not negligible [2]: In data of congested traffic measured near the bottleneck causing the breakdown, one often observes that, after the initial drop of the traffic flow, the flow decreases further during the first 10–20 min after the breakdown, cf., e.g., Fig. 12 in [24]. Assuming that, after the breakdown, the length of the congested area behind the bottleneck and thus the waiting time of each driver increases, gradual adaptation can naturally account for the observations. Figure 6 shows this effect in the simulated measurement of a virtual detector near the downstream congestion front. To average over fluctuations, we have chosen 3-min instead of one-minute sampling intervals for this figure. Extended congested traffic is simulated between $t = 60$ min and

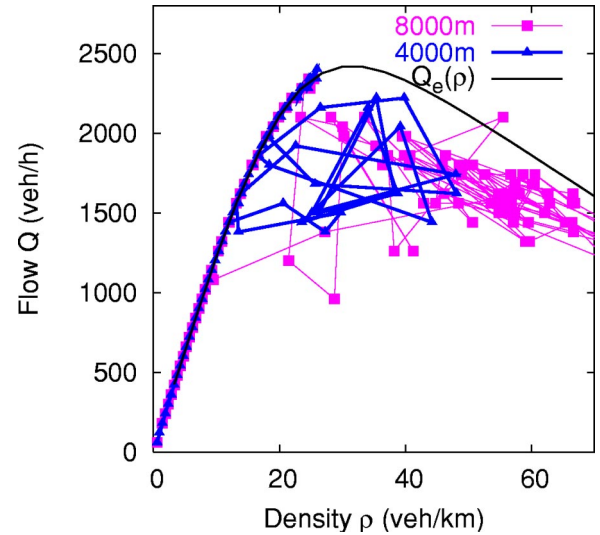


FIG. 7. Flow-density plot as in Fig. 3, simulated with the IDM without memory effects. To obtain the same degree of capacity and stability, the parameters T and a have been changed to 1.05 s and 1 m/s², respectively.

$t = 170$ min. The average flow is the highest in the beginning ($Q_{\text{cong}} \approx 1450$ veh/h at $t = 60$ min) and decreases to a minimum of below 1300 veh/h at about $t = 120$ min. At this time, the length of the congested region reaches its maximum value of about 10 km. Afterwards, when the congested area shrinks, the congested flow remains constant for some time before it increases by about 100 veh/h during the last 15 min of congestion ($155 \text{ min} \leq t \leq 170 \text{ min}$).

C. Comparison with the IDM

The question arises to which extent (i) the wide scattering, (ii) the distinct hysteresis effects indicated by the ratios Q_{\max}/Q_{CT} and Q_{\max}/Q_{jam} , and (iii) the low values of the “measured” densities in congested and jammed traffic are new features of the IDMM or occur in the original IDM without memory effects as well. Figure 7 shows a simulation with the original IDM, which is a special case of the IDMM for $\beta_T = 1$. The virtual detectors display scattering as well. However, the hysteresis effects are much smaller and the density of congested traffic is shifted to higher values, which are, in particular, higher than the values usually observed in empirical data.

IV. DISCUSSION

We have modeled a memory effect in the behavior of drivers by coupling existing car-following models to dynamical equations for some model parameters such as the minimum (safe) time gap T , the desired velocity v_0 , or the typical acceleration a . In this paper, we have used the IDM as the underlying model resulting in the IDMM, the “IDM with memory.” The Gipps model [35] seems to be a suitable candidate as well. It should be straightforward to apply the same concept to macroscopic models such as the gas-kinetic-based traffic (GKT) model [14,36] and to cellular automata. In fact, the slow-to-start rule [37] can be interpreted as the

special case of an instantaneous adaptation ($\tau=0$), which is only effective for standing traffic, i.e., the corresponding “level-of-service function,” Eq. (5), would be given by $\lambda_0(v)=1$ for $v>0$ and $\lambda_0(v)=0$ for $v=0$.

The concept could be also generalized to include the traffic density or the velocity variance in determining the level-of-service function. This would allow to model different kinds of adaptation behavior to different types of congested traffic such as homogeneous congested traffic and oscillating congested traffic (OCT) [34].

As is the case for the IDM, the IDMM is a deterministic car-following model with a unique fundamental diagram. It has two new parameters, the adaptation factor β_T and the adaptation time τ , which can be estimated from single-vehicle data. Simulations with the IDMM suggest that the adaptation of drivers to the surrounding traffic occurs on time scales of a few minutes and plays an important role in explaining the inverse- λ shape and the wide scattering of flow-density data in the congested regime measured by stationary detectors. Despite its simplicity, the model seems to be accurate enough to enable a direct analysis of the conventional interpretation of macroscopic flow-density data with surprising results both for the theoretician and the practitioner.

For the theoretician, probably the most interesting result is the direct demonstration of a simple mechanism that can explain the much-discussed wide scattering of congested traffic by longitudinal traffic instabilities. Important for the practitioner, the results suggest that the real traffic situation, in terms of the traffic density, is often worse than the macroscopic density data suggest. The resulting oscillations and even short periods of standing traffic are hidden in the “scattering” of the data. In contrast to previous results guided by theoretical considerations [5], the simulations suggest that congested traffic is nearly always unstable. This is supported by our analysis of more than 300 empirical examples of congestion from various freeways with a new visualization tool [38]. The majority of all congested traffic patterns originated

from a bottleneck (typically, an on-ramp) and displayed stop-and-go waves, many of them with growing amplitudes in time. Another factor obscuring the instability of real congested traffic is the often observed *convective* stability, which implies perturbations that can only propagate upstream, resulting in homogeneous congested traffic of high density near the downstream front of congestion (cf. the “pinch effect”) [1,14,33]. It should be pointed out that empirical studies of traffic data on Canadian freeways came to the conclusion that upstream propagating oscillations in congested traffic exist, but do not grow in amplitude [39]. Possibly this is related to different parameters characterizing driver-vehicle behavior on American freeways compared to European ones.

In our simulations, we have excluded most sources that would not surprise to produce scattering: We have not assumed heterogeneous multilane traffic exposed to fluctuation effects. Instead, we have assumed identical vehicles on a single lane with a dynamics given by a deterministic model with a unique fundamental diagram. We do not claim, however, that longitudinal instabilities and the memory effect would be the only causes leading to the observed scattering. Obviously, heterogeneous traffic plays a role as well. Furthermore, the role of lane changes remains to be investigated. Finally, it should be emphasized that we have investigated macroscopic implications of a microscopic model. To explain microscopic statistical properties such as the observed scaling law for the fluctuations of sample-average time headways [22], one probably needs to simulate both heterogeneous and multilane traffic. Microscopic statistical properties will be investigated in a forthcoming paper.

ACKNOWLEDGMENTS

The authors would like to acknowledge financial support by the DFG (Grant No. He 2789) and thank Arne Kesting for providing Fig. 1. We are also grateful to the Dutch Ministry of Transport, Public Works and Water Management for providing the single-vehicle induction-loop-detector data.

-
- [1] D. Helbing, *Rev. Mod. Phys.* **73**, 1067 (2001).
 - [2] *Traffic and Granular Flow'01: Social, Traffic, and Granular Dynamics*, edited by M. Fukui, Y. Sugiyama, M. Schreckenberg, and D.E. Wolf (Springer, Berlin, 2003).
 - [3] B.S. Kerner and H. Rehborn, *Phys. Rev. E* **53**, R4275 (1996).
 - [4] B.S. Kerner and H. Rehborn, *Phys. Rev. Lett.* **79**, 4030 (1997).
 - [5] B.S. Kerner, *Phys. Rev. E* **65**, 046138 (2002).
 - [6] P. Nelson, *Phys. Rev. E* **61**, R6052 (2000).
 - [7] R. Wiedemann, *Simulation des Straßenverkehrsflusses*, Schriftenreihe des IfV Vol. 8 (Universität Karlsruhe, Karlsruhe, Germany, 1974).
 - [8] A. Namazi, N. Eissfeldt, and A. Schadschneider, *Eur. Phys. J. B* **30**, 559 (2002).
 - [9] B.S. Kerner and S.L. Klenov, *J. Phys. A* **35**, L31 (2002).
 - [10] D. Helbing, D. Batic, M. Schönhof, and M. Treiber, *Physica A* **303**, 251 (2002).
 - [11] B.S. Kerner, S.L. Klenov, and D. Wolf, *J. Phys. A* **35**, 9971 (2002).
 - [12] W. Brilon and M. Ponzlet, in *Traffic and Granular Flow*, edited by D.E. Wolf, M. Schreckenberg, and A. Bachem (World Scientific, Singapore, 1996), pp. 23–40.
 - [13] S. Krauß, DLR, Report No. 98-08, 1998 (unpublished).
 - [14] M. Treiber and D. Helbing, e-print cond-mat/9901239.
 - [15] H. Lenz, C. Wagner, and R. Sollacher, *Eur. Phys. J. B* **7**, 331 (1998).
 - [16] W. Knosp, L. Santen, A. Schadschneider, and M. Schreckenberg, *Phys. Rev. E* **65**, 015101 (2001).
 - [17] I. Lubashevsky, R. Mahnke, P. Wagner, and S. Kalenkov, *Phys. Rev. E* **66**, 016117 (2002).
 - [18] J.H. Banks, An Investigation of Some Characteristics of Congested Flow, 1998 (unpublished).
 - [19] M. Treiber and D. Helbing, *J. Phys. A* **32**, L17 (1999).
 - [20] B. Tilch and D. Helbing, in *Traffic and Granular Flow'99*, edited by D. Helbing, H. Herrmann, M. Schreckenberg, and D. Wolf (Springer, Berlin, 2000), pp. 333–338.

- [21] L. Neubert, L. Santen, A. Schadschneider, and M. Schreckenberg, in *Traffic and Granular Flow'99* (Ref. [20]), pp. 307–314.
- [22] K. Nishinari, M. Treiber, and D. Helbing, e-print cond-mat/0212295 (2002).
- [23] M. Treiber, A. Hennecke, and D. Helbing, in *Traffic and Granular Flow'99* (Ref. [20]), pp. 365–376.
- [24] M. Treiber, A. Hennecke, and D. Helbing, Phys. Rev. E **62**, 1805 (2000).
- [25] L. Edie and R. Foote, in *Highway Research Board Proceedings, 37th Annual Meeting*, edited by H. Orland (National Academy of Sciences, Washington D.C., 1958).
- [26] P. de Gennes, *Scaling Concepts in Polymer Physics* (University Press, Cambridge, 1979).
- [27] S. Fedotov and Y. Okuda, Phys. Rev. E **66**, 021113 (2002).
- [28] M. Schulz, S. Trimper, and B. Schulz, Phys. Rev. E **64**, 026104 (2001).
- [29] W. Knosp, L. Santen, A. Schadschneider, and M. Schreckenberg, Phys. Rev. E **65**, 056133 (2002).
- [30] D. Helbing and M. Treiber, Comput. Sci. Eng. **1**, 89 (1999).
- [31] Remarkably, this simple scheme turned out to be more effective than standard fourth-order Runge-Kutta steps.
- [32] D. Helbing, A. Hennecke, V. Shvetsov, and M. Treiber, Math. Comput. Modell. **35**, 517 (2002).
- [33] B.S. Kerner, Phys. Rev. Lett. **81**, 3797 (1998).
- [34] D. Helbing, A. Hennecke, and M. Treiber, Phys. Rev. Lett. **82**, 4360 (1999).
- [35] P.G. Gipps, Transp. Res., Part B: Methodol. **15**, 105 (1981).
- [36] M. Treiber, A. Hennecke, and D. Helbing, Phys. Rev. E **59**, 239 (1999).
- [37] R. Barlovic, L. Santen, A. Schadschneider, and M. Schreckenberg, *Traffic and Granular Flow'97* (Springer, Singapore, 1998), p. 335.
- [38] M. Treiber and D. Helbing, Cooper@tive Tr@nsport@tion Dyn@mics **1**, 3.1 (2002), (Internet Journal, www.TrafficForum.org/journal); D. Helbing, Physik Journal **2**(5), 35 (2003); D. Helbing, in *Encyclopedia of Nonlinear Science*, edited by Alwyn Scott (Fitzroy Dearborn, London, in press); M. Schönhof and D. Helbing (unpublished); C. Drösser (unpublished).
- [39] M. Mauch and M.J. Cassidy, in *International Symposium of Traffic and Transportation Theory*, edited by M. Taylor (Elsevier, Amsterdam, 2002).